nature nanotechnology

ARTICLES

PUBLISHED ONLINE: 3 APRIL 2011 | DOI: 10.1038/NNANO.2011.41

Silica and titanium dioxide nanoparticles cause pregnancy complications in mice

Kohei Yamashita[1,2†], Yasuo Yoshioka[1,2,3†*], Kazuma Higashisaka[1,2], Kazuya Mimura[4], Yuki Morishita[1,2], Masatoshi Nozaki[4], Tokuyuki Yoshida[1,2], Toshinobu Ogura[1,2], Hiromi Nabeshi[1,2], Kazuya Nagano[2], Yasuhiro Abe[2], Haruhiko Kamada[2,3], Youko Monobe[5], Takayoshi Imazawa[5], Hisae Aoshima[6], Kiyoshi Shishido[7], Yuichi Kawai[8], Tadanori Mayumi[8], Shin-ichi Tsunoda[2,3,9], Norio Itoh[1], Tomoaki Yoshikawa[1,2], Itaru Yanagihara[4], Shigeru Saito[10] and Yasuo Tsutsumi[1,2,3*]

The increasing use of nanomaterials has raised concerns about their potential risks to human health. Recent studies have shown that nanoparticles can cross the placenta barrier in pregnant mice and cause neurotoxicity in their offspring, but a more detailed understanding of the effects of nanoparticles on pregnant animals remains elusive. Here, we show that silica and titanium dioxide nanoparticles with diameters of 70 nm and 35 nm, respectively, can cause pregnancy complications when injected intravenously into pregnant mice. The silica and titanium dioxide nanoparticles were found in the placenta, fetal liver and fetal brain. Mice treated with these nanoparticles had smaller uteri and smaller fetuses than untreated controls. Fullerene molecules and larger (300 and 1,000 nm) silica particles did not induce these complications. These detrimental effects are linked to structural and functional abnormalities in the placenta on the maternal side, and are abolished when the surfaces of the silica nanoparticles are modified with carboxyl and amine groups.

Nanomaterials such as nanosilica particles (nSPs), titanium dioxide nanoparticles (nano-TiO_2) and carbon nanotubes are already being applied in electronics[1], foods[2], cosmetics[3] and drug delivery[4]. nSPs are used as additives in cosmetics and foods because they are highly hydrophilic, easy to synthesize and their surfaces can be modified easily[5,6]. The increasing use of nanomaterials has raised concerns[7–9] because of recent reports showing that carbon nanotubes can induce mesothelioma-like lesions in mice, similar to those induced by asbestos[10,11]. We have also shown that nSPs can induce severe liver damage in mice and inflammatory responses *in vitro*[12,13].

Fetuses are known to be more sensitive to environmental toxins than adults[14–16], and it has been suggested that many chemical toxins in air, water and foods can induce pregnancy complications in humans[15,16]. An estimated 1 to 3% of women in the USA suffer recurrent miscarriages[17] and 7–15% of pregnancies are affected by poor fetal growth (a condition known as intrauterine growth restriction, IUGR)[18]. IUGR, which refers to a fetus with a weight below the 10th percentile for its gestational age, can cause fetal death and predisposes the child to a lifelong increased risk for cardiovascular disorders and renal disease[19,20]. Examining the potential risk of nanomaterials for causing miscarriage and IUGR is therefore essential.

Although some studies have shown transplacental transport of nanomaterials in pregnant animals and nanomaterial-induced neurotoxicity in their offspring[21–26], the effects of nanomaterials on pregnant animals have not yet been studied. Here, we investigated the biodistribution and fetotoxicity of various sizes of surface-modified nSPs, fullerene C_{60} and nano-TiO_2 in pregnant mice. Our results indicate that nSPs with diameters less than 100 nm and nano-TiO_2 with diameters of 35 nm induce resorption of embryos and fetal growth restriction. Furthermore, we found that modifying the surface of nSPs from –OH to –COOH or $-NH_2$ functional groups can prevent these pregnancy complications. These data include basic information regarding possible ways of creating safer nanomaterials.

Biodistribution of nanoparticles

Silica particles are well suited for studying the influence of nanomaterial size on biodistribution and various biological effects because they show much better dispersibility in aqueous solutions than most other nanomaterials[27]. We used silica particles with diameters of 70 nm (nSP70), 300 nm (nSP300) and 1,000 nm (mSP1000) to study the effect of size on biodistribution of the particles in pregnant mice. Two other common nanomaterials, nano-TiO_2 and fullerene, were also examined. All silica nanoparticles were confirmed by transmission electron microscopy (TEM) to be smooth-surfaced spheres (Supplementary Fig. S1a,b,c,g,h,i)[12,13]. The hydrodynamic diameters of nSP70, nSP300, mSP1000, nano-TiO_2 and fullerene were 65, 322, 1,140, 217 and 143 nm, respectively, with zeta

[1]Department of Toxicology and Safety Science, Graduate School of Pharmaceutical Sciences, Osaka University, 1-6 Yamadaoka, Suita, Osaka 565-0871, Japan, [2]Laboratory of Biopharmaceutical Research, National Institute of Biomedical Innovation, 7-6-8, Saito-Asagi, Ibaraki, Osaka 567-0085, Japan, [3]The Center for Advanced Medical Engineering and Informatics, Osaka University, 1-6, Yamadaoka, Suita, Osaka 565-0871, Japan, [4]Department of Developmental Medicine, Osaka Medical Center and Research Institute for Maternal and Child Health, 840 Murodo-cho, Izumi, Osaka 594-1101, Japan, [5]Bioresources Research, Laboratory of Common Apparatus, National Institute of Biomedical Innovation, 7-6-8, Saito-Asagi, Ibaraki, Osaka 567-0085, Japan, [6]Vitamin C60 BioResearch Corporation, 1-3-19, Yaesu, Chuo-ku, Tokyo 103-0028, Japan, [7]Mitsubishi Corporation, 2-6-1, Marunouchi, Chiyoda-ku, Tokyo 100-8086, Japan, [8]Graduate School of Pharmaceutical Sciences, Kobe-Gakuin University, 1-1-3, Minatojima, Chuo-ku, Kobe, Hyogo 650-8586, Japan, [9]Department of Biomedical Innovation, Graduate School of Pharmaceutical Sciences, Osaka University, 7-6-8 Saito-asagi, Ibaraki, Osaka 567-0085, Japan, [10]Department of Obstetrics and Gynecology, University of Toyama, 2630, Sugitani, Toyama 930-0194, Japan; †These authors contributed equally to this work.
*e-mail: yasuo@phs.osaka-u.ac.jp; ytsutsumi@phs.osaka-u.ac.jp

potentials of −53, −62, −67, −23 and −13 mV, respectively (see Supplementary Fig S2 for the physicochemical properties of all the materials). The size distribution spectrum of each silica particle showed a single peak (Supplementary Fig. S1m), and the hydrodynamic diameter corresponded almost precisely to the primary particle size for each sample (Supplementary Figs S1m and S2), indicating that the silica particles used in this study were well-dispersed in solution.

We examined the relationship between particle size and biodistribution in the placenta by whole-body imaging analysis after intravenous injection (through the tail vein) of fluorescent DY-676-labelled nSP70, nSP300 or mSP1000 into pregnant mice at gestational day 16 (GD16). At 24 h post-injection, intense fluorescence was observed in the liver of all mice receiving the differently sized nanoparticles (Fig. 1a), suggesting that the accumulation of nanoparticles in the liver is independent of size. Fluorescence was seen in the placenta of mice treated with nSP70, but not in mice treated with nSP300 or mSP1000 (Fig. 1a). We confirmed that ~5% of fluorescent DY-676 dissociated from the silica particles after *in vitro* incubation in phosphate buffered saline (PBS) for 24 h at 37 °C (Supplementary Fig. S1n), and no fluorescence was detected in the placenta of mice treated with fluorescent DY-676 only (data not shown), indicating that the fluorescence observed in the mice was caused by silica particle accumulation in the tissues.

TEM analysis revealed that nSP70 (nanosized spherical black objects in Fig. 1b–g) were found in placental trophoblasts (Fig. 1b,c), fetal liver (Fig. 1d,e) and fetal brain (Fig. 1f,g). No particles were seen in the placenta, fetal liver or fetal brain of mice treated with nSP300 or mSP1000 (data not shown). These results suggest that the biodistribution of silica particles varied according to particle size, and that only the smaller nSP70 nanoparticles accumulated in the placenta and fetus. Similarly, nano-TiO_2 were found in placental trophoblasts (Fig. 1h,i), the fetal liver (Fig. 1j,k) and fetal brain (Fig. 1l,m) after intravenous injection into pregnant mice. We did not evaluate the biodistribution of fullerene C_{60} because of the difficulty in detecting fullerene using TEM.

Recently, several reports have shown that some nanomaterials can penetrate mouse and *ex vivo* human placental tissue[25,28], and it is generally known that high-molecular-weight species (>1,000 Da) do not penetrate the placenta by passive diffusion. Thus, we speculated that nSP70 either directly injured the blood–placenta barrier or was actively transported through it, or both. Furthermore, nSP70 in the fetal circulation would have access to the fetal liver and brain, because the development of the blood–brain barrier in the fetal brain is incomplete[29].

Fetotoxicity of nanoparticles

To determine the fetotoxicity of nSP70, nSP300, mSP1000, nano-TiO_2 and fullerene in pregnant mice, we intravenously injected the particles (100 μl, 0.8 mg per mouse) into pregnant mice on two consecutive days, at GD16 and GD17, and measured the maternal blood biochemistry. None of the silica particles induced any significant changes in the levels of aspartate aminotransferase (AST), alanine aminotransferase (ALT) and blood urea nitrogen (BUN), and all parameters remained within the physiological range, indicating that the particles did not induce maternal liver and kidney damage at the administered doses (Supplementary Fig. S3). Blood pressure and heart rates among all groups of mice that received silica nanoparticles were similar and comparable to control animals receiving PBS (Supplementary Fig. S4). However, there was a significant increase in the number of granulocytes in nSP70-treated pregnant mice compared with control mice receiving PBS (Supplementary Fig. S5).

When compared to control mice, the maternal body weight of nSP70- and nano-TiO_2-treated mice decreased at GD17 and GD18, whereas those treated with nSP300, mSP1000 and fullerenes did not show any changes (Fig. 2a). Mice that received nSP70 and nano-TiO_2 had 20% and 30% lower uterine weights (Fig. 2b,c), respectively, and significantly higher fetal resorption rates than control mice and those that received nSP300, mSP1000 particles or fullerene (Fig. 2d). nSP70- and nano-TiO_2-treated mice also had smaller fetuses (nearly 10% lower than control mice, Fig. 2e,g) and smaller amnion sacs than mice that received nSP300, mSP1000 or fullerene.

In contrast, the weights of placentae were the same among all groups of mice (Fig. 2f,h). When mice were injected with lower concentrations of nSP70 (0.2 and 0.4 mg per mouse), none of the above symptoms was observed; fetal resorption and growth restriction were seen only at the highest dose used (0.8 mg per mouse; Supplementary Fig. S6). These results indicate that only nSP70 at the highest concentration and nano-TiO_2 induced fetal resorption and restricted fetal growth; fullerene did not induce any pregnancy complications. The doses used here are typical of preclinical studies for drug delivery applications of silica particles, intravenously administered at several hundred milligrams per mouse[30]. In contrast, the most common route of nano-TiO_2 exposure to humans is through the skin (for example, through the application of nano-TiO_2-containing cosmetics) and some reports have suggested that nano-TiO_2 particles do not penetrate into living skin[31,32]. Therefore, we believe that nano-TiO_2 may not induce any pregnancy complications following topical application. Furthermore, we have confirmed that the nano-TiO_2 used in this study did not induce cellular toxicity and DNA damage *in vitro* (data not shown).

It is known that the surface properties of nanomaterials can influence biodistribution, inflammatory responses and cellular toxicity[27,33]. We examined the relationship between fetotoxicity and the surface properties of nSP70. The nSP70 was surface-modified with COOH or NH_2 functional groups (nSP70-C or nSP70-N, respectively), and both were confirmed by TEM to be smooth-surfaced spherical particles (Supplementary Fig. S1). The hydrodynamic diameters of the nSP70-C and nSP70-N were 70 and 72 nm, respectively, with zeta potentials of −76 and −29 mV, respectively, indicating that surface modification changed the surface charge of the particles (Supplementary Fig. S2).

As with nSP70, mice that were intravenously injected with DY-676-labelled nSP70-C and nSP70-N showed fluorescence in the placenta (Fig. 1a). TEM analysis revealed that nSP70-C and nSP70-N were found in placental trophoblasts (Fig. 1n,q), fetal liver (Fig. 1o,r) and fetal brain (Fig. 1p,s), indicating that the particles accumulated in the placenta and fetus. The maternal body weights of mice treated with nSP70-C or nSP70-N were the same as those observed for control mice (Fig. 2a). nSP70-C and nSP70-N did not affect the uterine weight (Fig. 2c), fetal weight (Fig. 2e,g) or fetal resorption rate (Fig. 2b,d). These results suggest that modifying the surface of nSP70 can prevent resorption and fetal growth restriction induced by nSP70.

Placental dysfunction in nSP70-treated mice

Normal placental development is required for embryonic growth, and placental dysfunction has been associated with miscarriage and fetal growth restriction[34,35]. The mature murine placenta consists of four layers: maternal decidua, trophoblast giant cell, spongiotrophoblast and labyrinth[34,35] (Fig. 3a). Maternal spiral arteries converge into canals between the trophoblast giant cells, and these canals pass through the spongiotrophoblast and labyrinth layers[34,35]. The exchange of respiratory gases, nutrients and waste takes place in the labyrinth layer between the fetal blood vessels and maternal blood sinuses[34,35].

To clarify the relationship between particle size, fetotoxicity and placental dysfunction, we examined the pathological histology of the placenta in nSP-treated mice using haematoxylin and eosin (H&E) staining (Fig. 3b–e). The placenta of mice treated with nSP70 showed variable structural abnormalities, whereas those treated

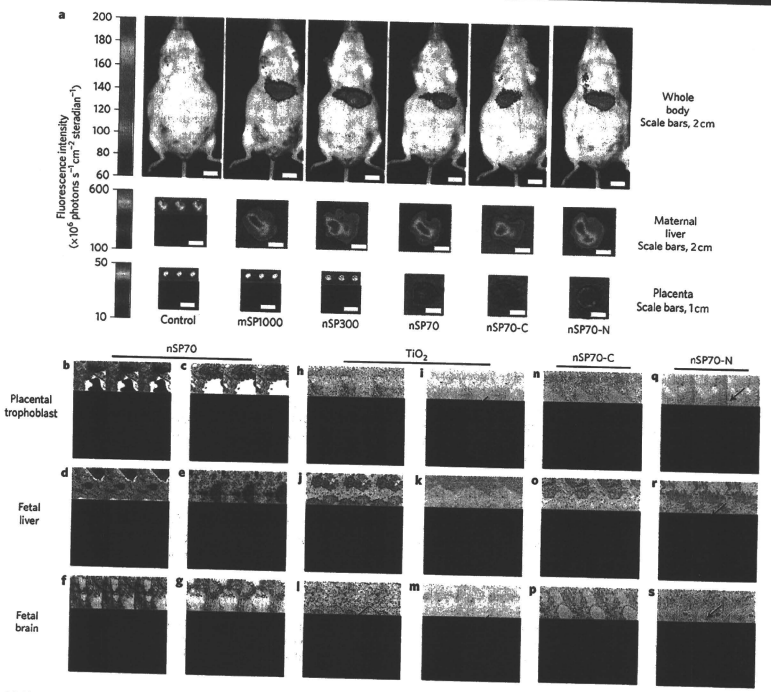

Figure 1 | Biodistribution of nanoparticles in pregnant mice. a, *In vivo* fluorescence images. Pregnant mice at GD16 were treated with 0.8 mg DY-676-labelled silica particles per mouse (nSP70, nSP300, mSP1000, nSP70-C or nSP70-N) or PBS (control), intravenously, through the tail vein. After 24 h, optical images of the whole body, maternal liver and placenta were acquired with a Xenogen IVIS 200 imaging system. **b–s**, TEM images of placentae and fetuses at GD18. Pregnant mice were treated intravenously with 0.8 mg per mouse of nSP70, nano-TiO_2, nSP70-C or nSP70-N on two consecutive days (GD16 and GD17). Arrows indicate nanoparticles. These particles were present in placental trophoblast cells (**b,c,h,i,n,q**), fetal liver cells (**d,e,j,k,o,r**) and fetal brain cells (**f,g,l,m,p,s**).

with nSP300 and mSP1000 did not show any significant abnormalities when compared to control mice (Fig 3b,d). Spiral artery canals failed to form (Fig. 3b,d) and blood flow was reduced in the fetal vascular sinuses of nSP70-treated mice (Fig. 3c,e). To further elucidate the influence of nanoparticles on placental dysfunction, we are examining the pathological histology of the placenta in nano-TiO_2-treated mice at present.

The areas including the placental major layers (the spongiotrophoblast and labyrinth) in nSP70-treated and control mice were examined by periodic acid–Schiff (PAS) staining (Fig. 3f–i). The total areas of placentae from each nSP70-treated mouse were not significantly different from those of control mice (Fig. 4a). The area of the spongiotrophoblast layer (Fig. 4b) and the ratio of the spongiotrophoblast layer area to the total placental area (Fig. 4c) in nSP70-treated mice were almost 50% smaller than those observed in control mice. The percentage of nuclei positively stained by terminal transferase-mediated dUTP nick end-labelling (TUNEL) was significantly higher within the spongiotrophoblast layer of nSP70-treated mice than within that of control mice, indicating that nSP70 induced apoptotic cell death of spongiotrophoblasts (Fig. 3j,k; Fig. 4d). The surrounding lengths of the villi in the labyrinth layer of nSP70-treated mice were significantly decreased compared to those of control mice (Fig. 3l,m; Fig. 4f), whereas the ratio of the labyrinth layer area to the total placental area in nSP70-treated mice was not significantly different from that of control mice (Fig. 4e). These results suggest that nSP70-induced pregnancy complications were probably caused by placental cellular damage, which might affect maternal–fetal exchange.

Normal placental development requires the coordinated expression of vascular endothelial growth factor (VEGF) and its receptor, fms-like tyrosine kinase-1 (Flt-1)[36]. Soluble Flt-1 (sFlt-1) is expressed by placental cells including spongiotrophoblasts, and is a potent anti-angiogenic molecule that regulates the generation of placental vasculature during pregnancy by sequestering circulating VEGF and regulating the action of VEGF[37]. The plasma level of sFlt-1 in nSP70- and nano-TiO_2-treated mice was significantly

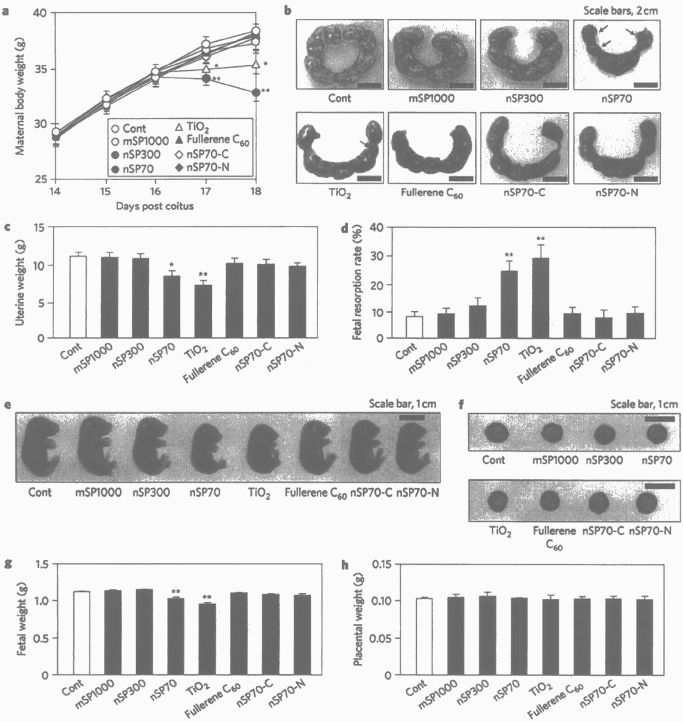

Figure 2 | Pregnancy complications in nSP70- or nano-TiO_2-treated mice. Pregnant mice were treated intravenously with 0.8 mg per mouse of nSP70, nSP300, mSP1000, nano-TiO_2, fullerene C_{60}, nSP70-C, nSP70-N or PBS (control) on two consecutive days (GD16 and GD17). **a**, Changes in maternal body weight. Maternal body weights were evaluated daily ($n = 11$–24). Statistically significant difference from control mice, $^*P < 0.05$ and $^{**}P < 0.01$ by ANOVA. **b–h**, Pregnancy complications. Uteri from mice were excised at GD18 (**b**). Uterine weights (**c**) and fetal resorption rates (**d**) were evaluated ($n = 11$–24). Fetuses (**e**) and placentae (**f**) were excised from uteri. Fetal weights (**g**) and placental weights (**h**) were evaluated ($n = 37$–212). All data represent means ± s.e.m ($^*P < 0.05$, $^{**}P < 0.01$ versus value for control mice by ANOVA).

lower than in control mice and those receiving nSP300, mSP1000, fullerene, nSP70-C and nSP70-N (Supplementary Fig. S7a–d), indicating that nSP70 induced not only structural abnormalities, but also functional abnormalities, in the mouse placenta.

The anticoagulation agent heparin is often administered to prevent miscarriage and IUGR[38]. Mice treated with a combination of nSP70 and heparin had slightly increased maternal body weights and decreased fetal resorption rates compared to mice that were not treated with heparin (Fig. 5a,c). Heparin treatment prevented decreases in uterine and fetal weight in nSP70-treated mice (Fig. 5b,d). Mice treated with a combination of nSP70 and heparin had similar levels of sFlt-1 to control mice (Supplementary Fig. S7e). These results suggest that the mechanism for nSP70-induced pregnancy complications might involve coagulation. However, it has recently been shown that heparin acts in many ways other than as an anticoagulant[39–42]. The anti-complement activation effect of heparin has been suggested to be important in mitigating pregnancy complications[40]. Complement activation induces neutrophil activation and this may lead to placental dysfunction, miscarriage, fetal growth restriction or pre-eclampsia[43,44]. Here, we have shown that the number of granulocytes in nSP70-treated mice is significantly higher than in control mice (Supplementary Fig. S5), indicating that nSP70 might have induced complement activation, which may have subsequently activated neutrophils and systemic inflammation.

Some reports have shown that heparin may also act as a placental growth factor, because heparin is known to inhibit placental apoptosis, stimulate placental proliferation and enhance the effect of several growth factors[39,41,42]. Moreover, oxidative stress in the placenta is known to cause placental dysfunction and to induce pregnancy

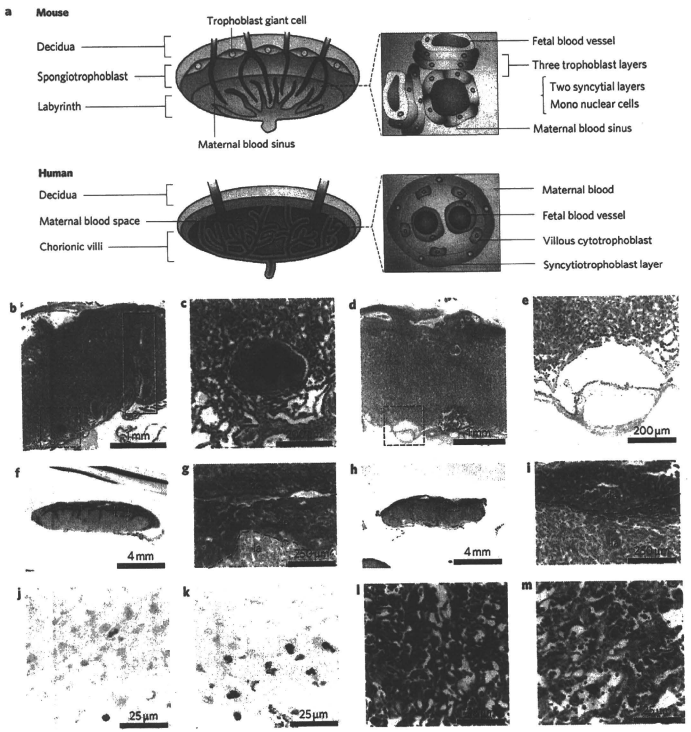

Figure 3 | Pathological examination of placenta. a, Schematic showing the differences between human and mouse placentae. **b–m**, Histological examination. Pregnant mice were treated intravenously with 0.8 mg per mouse of nSP70 or PBS (control) on two consecutive days (GD16 and GD17). At GD18, sections of placentae from PBS- (**b,c,f,g**) or nSP70-treated mice (**d,e,h,i**) were stained with H&E (**b–e**) or PAS (**f–i**). The solid box in **b** indicates the presence of spiral arteries and canals. Panels **c**, **e**, **g**, and **i** are enlarged images of the areas within the dashed boxes in **b**, **d**, **f** and **h**, respectively. In **g** and **i**, dashed lines delineate the decidua (de), spongiotrophoblast layer (sp) and labyrinth layer (la). Spongiotrophoblast layers of PBS- (**j**) or nSP70-treated mice (**k**) were stained with TUNEL. Labyrinth layers of PBS- (**l**) or nSP70-treated mice (**m**) were stained with H&E.

complications[45]. Nanomaterials have been reported to cause oxidative stress, which in turn induces cell apoptosis and inflammation[22,46,47]. Therefore, the pregnancy complications observed here might have been caused by oxidative stress induced by nSP70.

We have observed that the induction of oxidative stress in cells and the activation of the coagulation pathway in mice treated with nSP70-C and nSP70-N were lower than those observed in cells and mice treated with nSP70 (unpublished data). Therefore, we speculate that the lower activation of coagulation, complement and oxidative stress in the placenta of mice treated with nSP70-C and nSP70-N might have prevented pregnancy complications in those mice. It has recently been shown that nanomaterials become coated with serum proteins and induce different cellular responses by binding to proteins[48]. In addition, different surface characteristics, such as surface charge, are known to influence the binding affinities of proteins to nanomaterials[48]. Therefore, the differences in protein binding among nSP70, nSP70-C and nSP70-N might have given rise to differences in the fetotoxicity of the nanomaterials.

It should be noted that there are differences between mouse and human placentae, such as the greater role of yolk sac placentation in the mouse and the anatomy in the labyrinth[49,50] (Fig. 3a). The yolk sac plays a significant role in material transport from mother to fetus in mice, especially before the placental circulation is established[49]. Therefore, the accumulation of nSP70 in the yolk sac should be investigated to understand the accumulation mechanism of nanoparticles in fetuses. In the mouse placenta, three trophoblast layers embrace the fetal vasculature in the labyrinth layer, whereas in the human term placenta, a single syncytial layer with an underlying trophoblast stem cell layer is present in the villi[49,50]. As these anatomical and structural differences might affect nanoparticle

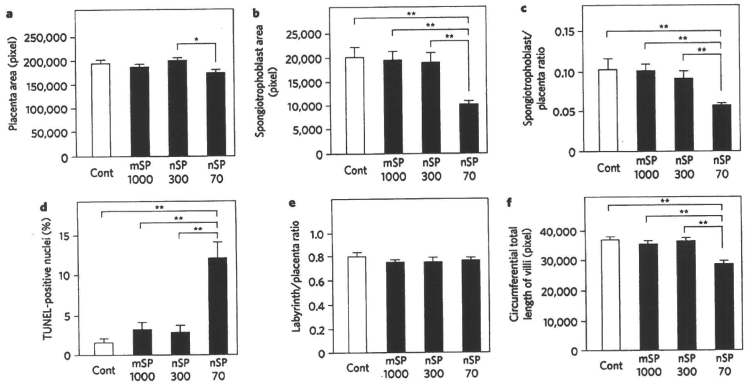

Figure 4 | Dysfunction of placentae. Pregnant mice were treated intravenously with 0.8 mg per mouse of nSP70, nSP300, mSP1000 or PBS (control) on two consecutive days (GD16 and GD17). **a–e**, At GD18, the area of the placenta (**a**) and the spongiotrophoblast layer (**b**) and the ratios of the spongiotrophoblast layer area to the total placental area (**c**) and of the labyrinth layer area to the total placental area (**e**) were assessed by examining the PAS-stained sections in Fig. 3f-i and were analysed quantitatively. The apoptotic index (**d**) was assessed by examining the TUNEL-stained sections in Fig. 3j,k and was quantitatively analysed. The surrounding length of the villi (**f**) in the labyrinth layers was assessed by examining the H&E-stained sections in Fig. 3l,m and was quantitatively analysed. All data represent means ± s.e.m. ($n = 11$–20; $^*P < 0.05$ and $^{**}P < 0.01$ by ANOVA).

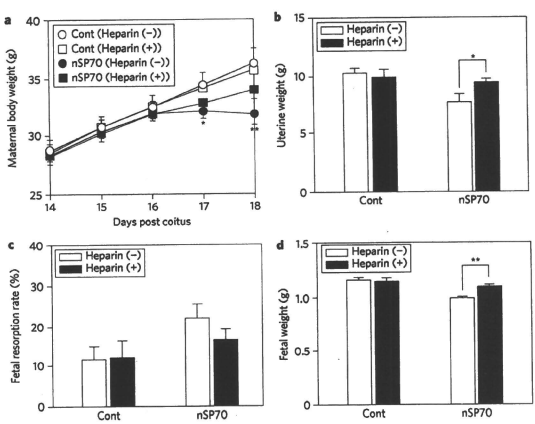

Figure 5 | Prevention of nSP70-induced pregnancy complications with heparin. Pregnant mice were treated intravenously with 0.8 mg per mouse of nSP70 or PBS (control) through the tail vein with or without heparin on two consecutive days (GD16 and GD17). **a**, Changes in maternal body weights. Maternal body weights were evaluated daily ($n = 10$–15). Statistically significant difference from control mice, $^*P < 0.05$ and $^{**}P < 0.01$ by ANOVA. **b–d**, Analysis of pregnancy complications in nSP70-treated mice with or without heparin treatment. At GD18, uterine weights (**b**), fetal resorption rates (**c**) and fetal weights (**d**) were evaluated (**b**,**c**, $n = 10$–15; **d**, $n = 55$–89). All data represent means ± s.e.m., $^*P < 0.05$ and $^{**}P < 0.01$ by Student's *t*-tests.

uptake and distribution, we cannot extrapolate our data about the placental distribution of nanoparticles, or placental dysfunction induced by nanoparticles, to humans. Additional studies that examine the penetration efficiency of nanoparticles into the human placenta (using *ex vivo* human placental tissue) are needed, as are studies that focus on the relationship between pregnancy complications and the amount of nanoparticles in the human placenta.

Conclusion

Of the materials studied here, nSP70 and nano-TiO_2 induced fetal resorption and restricted the growth of fetuses in pregnant mice, whereas fullerene C_{60} did not induce these complications. nSP70 and nano-TiO_2 were observed in the placenta, fetal liver and fetal brain, and nSP70 induced complications only at the highest concentration (0.8 mg per mouse) administered. The detrimental effects seen in nSP70-treated mice were linked to structural and functional changes in the placenta. Modification of the surface of nSP70 with carboxyl or amine groups abrogated the negative effects, suggesting the importance of surface charge. Although the nSP70 and nano-TiO_2 were mainly designed for experimental and industrial use, and not for cosmetics or food, we suggest that the potential fetotoxicity of these and other nanomaterials should be investigated more carefully.

Methods

Particles. nSP70, nSP300, mSP1000, nSP70-C and nSP70-N, as well as nSP70, nSP300 and mSP1000 labelled with DY-676 (excitation and emission wavelengths of 674 and 699 nm, respectively), were purchased from Micromod Partikeltechnologie. Rutile-type TiO_2 particles with a diameter of 35 nm (designated nano-TiO_2, Tayca Corporation) were also used. Polyvinylpyrrolidone (PVP)-wrapped fullerene C_{60} was provided by Vitamin C60 BioResearch Corporation. The nanoparticles were used after 5 min of sonication (280 W output (Ultrasonic Cleaner, AS One) and 1 min of vortexing.

Mice. Pregnant BALB/c mice (8–10 weeks) were purchased from Japan SLC. The experimental protocols conformed to the ethical guidelines of Osaka University and the National Institute of Biomedical Innovation, Japan.

***In vivo* imaging.** *In vivo* fluorescence imaging was performed with an IVIS 200 small-animal imaging system (Xenogen). At GD16, pregnant BALB/c mice were injected with 100 μl (0.8 mg per mouse) DY-676-labelled nSP70, nSP300, mSP1000, nSP70-C, nSP70-N or PBS (control), intravenously through the tail vein. At 24 h post-injection, the mice were anaesthetized, and images were obtained with a cy5.5 filter set (excitation/emission, 615–665 nm/695–770 nm). Imaging parameters were selected and implemented with Living Image 2.5 software (Xenogen).

TEM analysis. Pregnant BALB/c mice were treated with 100 μl (0.8 mg per mouse) of nSP70, nSP300, mSP1000, nSP70-C, nSP70-N or nano-TiO_2, intravenously through the tail vein, on two consecutive days (GD16 and GD17). At GD18, mice were killed after being anaesthetized, and the placenta, fetal liver and fetal brain were fixed in 2.5% glutaraldehyde for 2 h. Small pieces of tissue collected from these samples were washed with phosphate buffer, postfixed in sodium cacodylate-buffered 1.5% osmium tetroxide for 60 min at 4 °C, dehydrated using a series of ethanol concentrations, and embedded in Epon resin. The samples were examined under a Hitachi electron microscope (H-7650; Hitachi).

Fetotoxicity. Pregnant BALB/c mice were treated with 100 μl of nSP70 (0.2 mg, 0.4 mg or 0.8 mg per mouse), nSP300 (0.8 mg per mouse), mSP1000 (0.8 mg per mouse), nSP70-C (0.8 mg per mouse), nSP70-N (0.8 mg per mouse), nano-TiO_2 (0.8 mg per mouse), fullerene C_{60} (0.8 mg per mouse) or PBS (control), intravenously through the tail vein, on two consecutive days (GD16 and GD17). All mice were killed after being anaesthetized at GD18. Blood samples were collected in tubes containing 5 IU ml^{-1} heparin sodium, and plasma was harvested. The rate of fetal resorption was calculated (number of resorptions/total number of formed fetuses and resorptions). The fetuses and placentae of each mouse were excised and weighed, and the weight of the uterus calculated as the sum of the placental and fetal weights. To study the effects of heparin in nSP70-treated mice, pregnant BALB/c mice were treated with 100 μl (0.8 mg per mouse) nSP70 or PBS (control) intravenously through the tail vein on two consecutive days (GD16 and GD17). The same mice were treated with heparin (Sigma-Aldrich, 10 U) intraperitoneally on two consecutive days (GD16 and GD17), twice a day, 3 h before nSP70 treatment and 3 h after nSP70 treatment.

Histological examination. After fixing placentae in 10% formalin neutral buffer solution overnight, tissues were washed in PBS, dehydrated in a graded series of ethanol and xylene solutions, and embedded in paraffin. Sections (2 μm) were cut with a microtome. Sections were deparaffinized, rehydrated in a graded series of ethanols, and stained with H&E or PAS. Stained sections were dehydrated in a series of ethanols and mounted using permount. Representative histological images were recorded with a charge-coupled device (CCD) digital camera fixed to a microscope. The areas of the placenta, spongiotrophoblast layer and labyrinth layer were assessed by examining light microscopy images (Olympus) of the PAS-stained sections and were quantitatively analysed with Image J Imaging System Software Version 1.3 (National Institutes of Health). The circumferential total length of villi was assessed by examining light microscopy images of the H&E-stained sections and quantitatively analysed with Image J Imaging System Software Version 1.3. The presence of apoptotic cells in placental sections was analysed by TUNEL assay (Millipore). The tissue was counterstained with methyl green. Photographs of TUNEL (brown) and methyl green (light blue) staining were captured at three randomly selected fields in the spongiotrophoblast layer. TUNEL-positive nuclei (apoptotic nuclei) and methyl green-stained nuclei (total nuclei) were counted in the spongiotrophoblast layer. The apoptotic index in each section was calculated as the percentage of spongiotrophoblast nuclei stained TUNEL-positive divided by the total number of methyl green-stained nuclei found within the spongiotrophoblast layer.

Statistical analysis. All results are presented as means ± standard error of the mean (s.e.m.). Statistical significance in the differences was evaluated by Student's *t*-tests or Tukey's method after analysis of variance (ANOVA).

Received 23 September 2010; accepted 28 February 2011; published online 3 April 2011

References

1. Konstantatos, G. & Sargent, E. H. Nanostructured materials for photon detection. *Nature Nanotech.* **5**, 391–400 (2010).
2. Augustin, M. A. & Sanguansri, P. Nanostructured materials in the food industry. *Adv. Food. Nutr. Res.* **58**, 183–213 (2009).
3. Bowman, D. M., van Calster, G. & Friedrichs, S. Nanomaterials and regulation of cosmetics. *Nature Nanotech.* **5**, 92 (2010).
4. Petros, R. A. & DeSimone, J. M. Strategies in the design of nanoparticles for therapeutic applications. *Nature Rev. Drug Discov.* **9**, 615–627 (2010).
5. Martin, K. R. The chemistry of silica and its potential health benefits. *J. Nutr. Health Aging.* **11**, 94–97 (2007).
6. Knopp, D., Tang, D. & Niessner, R. Review: bioanalytical applications of biomolecule-functionalized nanometer-sized doped silica particles. *Anal. Chim. Acta.* **647**, 14–30 (2009).
7. Kagan, V. E., Bayir, H. & Shvedova, A. A. Nanomedicine and nanotoxicology: two sides of the same coin. *Nanomedicine* **1**, 313–316 (2005).
8. Nel, A., Xia, T., Madler, L. & Li, N. Toxic potential of materials at the nanolevel. *Science* **311**, 622–627 (2006).
9. Fadeel, B. & Garcia-Bennett, A. E. Better safe than sorry: understanding the toxicological properties of inorganic nanoparticles manufactured for biomedical applications. *Adv. Drug. Deliv. Rev.* **62**, 362–374 (2010).
10. Poland, C. A. *et al.* Carbon nanotubes introduced into the abdominal cavity of mice show asbestos-like pathogenicity in a pilot study. *Nature Nanotech.* **3**, 423–428 (2008).
11. Donaldson, K., Murphy, F. A., Duffin, R. & Poland, C. A. Asbestos, carbon nanotubes and the pleural mesothelium: a review of the hypothesis regarding the role of long fibre retention in the parietal pleura, inflammation and mesothelioma. *Part. Fibre Toxicol.* **7**, 5 (2010).
12. Nabeshi, H. *et al.* Systemic distribution, nuclear entry and cytotoxicity of amorphous nanosilica following topical application. *Biomaterials* **32**, 2713–2724 (2011).
13. Nabeshi, H. *et al.* Amorphous nanosilica induce endocytosis-dependent ROS generation and DNA damage in human keratinocytes. *Part. Fibre Toxicol.* **8**, 1 (2011).
14. Koren, G., Pastuszak, A. & Ito, S. Drugs in pregnancy. *N. Engl. J. Med.* **338**, 1128–1137 (1998).
15. Tardiff, R. G., Carson, M. L. & Ginevan, M. E. Updated weight of evidence for an association between adverse reproductive and developmental effects and exposure to disinfection by-products. *Regul. Toxicol. Pharmacol.* **45**, 185–205 (2006).
16. Wigle, D. T. *et al.* Epidemiologic evidence of relationships between reproductive and child health outcomes and environmental chemical contaminants. *J. Toxicol. Environ. Health. B. Crit. Rev.* **11**, 373–517 (2008).
17. Mills, J. L. *et al.* Incidence of spontaneous abortion among normal women and insulin-dependent diabetic women whose pregnancies were identified within 21 days of conception. *N. Engl. J. Med.* **319**, 1617–1623 (1988).
18. Cetin, I. & Alvino, G. Intrauterine growth restriction: implications for placental metabolism and transport. A review. *Placenta* **30(Suppl. A)**, S77–S82 (2009).
19. Godfrey, K. M. & Barker, D. J. Fetal nutrition and adult disease. *Am. J. Clin. Nutr.* **71**, 1344S–1352S (2000).
20. Barker, D. J. Adult consequences of fetal growth restriction. *Clin. Obstet. Gynecol.* **49**, 270–283 (2006).
21. Takeda, K. *et al.* Nanoparticles transferred from pregnant mice to their offspring can damage the genital and cranial nerve systems. *J. Health Sci.* **55**, 95–102 (2009).
22. Shimizu, M. *et al.* Maternal exposure to nanoparticulate titanium dioxide during the prenatal period alters gene expression related to brain development in the mouse. *Part. Fibre Toxicol.* **6**, 20 (2009).
23. Tian, F. *et al.* Surface modification and size dependence in particle translocation during early embryonic development. *Inhal. Toxicol.* **21(Suppl. 1)**, 92–96 (2009).
24. Saunders, M. Transplacental transport of nanomaterials. *Wiley Interdiscip. Rev. Nanomed. Nanobiotechnol.* **1**, 671–684 (2009).

胎盤と免疫

島　友子　　中島彰俊　　斎藤　滋

はじめに

母体にとってsemi-allograftである胎児が母体免疫機構から拒絶されずに妊娠が継続することは，未だ大きな謎である。最近の免疫学の進歩により，母体の免疫細胞，胎児，胎盤は巧妙にクロストークし，免疫寛容が成立し，妊娠維持につながることが証明されてきた。母児の境界面にある臓器である胎盤の中で胎児組織である絨毛細胞側では，母体免疫応答を避けるために標的分子となる移植抗原である主要組織適合性抗原(MHC抗原)の発現パターンを変化させている。また，母体側すなわち脱落膜の白血球組成は末梢血中の組成と大きく異なり，約70%をnatural killer(NK)細胞が占め，末梢血で主体となっているT細胞はわずか10～20%を占めているにすぎない。ほかに樹状細胞(1～2%)やマクロファージ(20%)が存在しているがB細胞はほとんど存在しない。母体側の免疫担当細胞の妊娠による変化も正常な妊娠維持に重要な役割を果たしている。したがって，これら免疫学的妊娠維持機構の破綻は原因不明の着床不全，反復流産や，妊娠高血圧腎症に関連づけられると考えられる。本稿では，胎盤における免疫機構について概説する。

胎児，胎盤と母体免疫とのかかわり：胎盤の抗原性(図1)

母体の子宮内に胚が着床し，胎盤が形成される。その後，胎盤の絨毛間腔に母体血が流れ込み，絨毛を介して母子間の栄養交換，酸素交換が行われる。その際，浮遊絨毛(villous trophoblast)は直接母体血液と接触するが，浮遊絨毛はCD8$^+$T細胞やNK細胞に認識されるMHCクラスⅠ抗原，CD4$^+$T細胞に認識されるクラスⅡ抗原ともに発現しておらず，免疫応答が起きにくいようになっている。一方，絨毛外トロホブラスト(extravillous trophoblast：EVT)は胎盤組織を子宮に固着させるために胎盤形成時に子宮筋層内に侵入する。また，EVTはらせん動脈の平滑筋を置換し動脈を拡張させ絨毛間腔への血流を増加させる。このEVTにもMHCクラスⅡ抗原は存在しないが，MHCクラスⅠ抗原であるHLA-C，およびMHCクラスⅠb抗原であるHLA-E，HLA-F，HLA-Gを発現している。

また，最近の研究では，胎盤のもつ解剖学的障壁は必ずしも完璧なものではなく，胎児と母体間には細胞の交通(microchimerism)が起こっているのが明らかとなっている。母体血液中には大量のシンシトロホブラストの小断片が循環しており，このトロホブラストの断片内の小胞体(endoplasmic reticulum)にはHLA-DRおよびDQといったMHCクラスⅡ抗原が発現されている。これらの胎児抗原は，母体の抗原提示細胞に取り込まれ，オートファジーを介してリソゾームへ輸送され，MHCクラスⅡ分子に提示される(cross presentation)ことも報告されている。母体の免疫系は胎児抗原を認識していることが次々と証明されている。

脱落膜におけるNK細胞の働き

哺乳類では妊娠すると，大型の顆粒をもつNK

しま ともこ，なかしま あきとし，さいとう しげる
富山大学産科婦人科
〒930-0194　富山県富山市杉谷2630
E-mail address：shitoko@med.u-toyama.ac.jp

25. Chu, M. *et al.* Transfer of quantum dots from pregnant mice to pups across the placental barrier. *Small* **6,** 670–678 (2010).
26. Hougaard, K. S. *et al.* Effects of prenatal exposure to surface-coated nanosized titanium dioxide (UV-Titan). A study in mice. *Part. Fibre Toxicol.* **7,** 16 (2010).
27. He, X. *et al. In vivo* study of biodistribution and urinary excretion of surface-modified silica nanoparticles. *Anal. Chem.* **80,** 9597–9603 (2008).
28. Wick, P. *et al.* Barrier capacity of human placenta for nanosized materials. *Environ. Health Perspect.* **118,** 432–436 (2010).
29. Watson, R. E., Desesso, J. M., Hurtt, M. E. & Cappon, G. D. Postnatal growth and morphological development of the brain: a species comparison. *Birth Defects Res. B. Dev. Reprod. Toxicol.* **77,** 471–484 (2006).
30. Li, L. *et al. In vivo* delivery of silica nanorattle encapsulated docetaxel for liver cancer therapy with low toxicity and high efficacy. *ACS Nano.* **4,** 6874–6882 (2010).
31. Filipe, P. *et al.* Stratum corneum is an effective barrier to TiO_2 and ZnO nanoparticle percutaneous absorption. *Skin Pharmacol. Physiol.* **22,** 266–275 (2009).
32. Sadrieh, N. *et al.* Lack of significant dermal penetration of titanium dioxide from sunscreen formulations containing nano- and submicron-size TiO_2 particles. *Toxicol. Sci.* **115,** 156–166 (2010).
33. Albrecht, C. *et al.* Inflammatory time course after quartz instillation: role of tumor necrosis factor-alpha and particle surface. *Am. J. Respir. Cell. Mol. Biol.* **31,** 292–301 (2004).
34. Kibschull, M., Gellhaus, A. & Winterhager, E. Analogous and unique functions of connexins in mouse and human placental development. *Placenta* **29,** 848–854 (2008).
35. Gasperowicz, M. & Otto, F. The notch signalling pathway in the development of the mouse placenta. *Placenta* **29,** 651–659 (2008).
36. Lam, C., Lim, K. H. & Karumanchi, S. A. Circulating angiogenic factors in the pathogenesis and prediction of preeclampsia. *Hypertension* **46,** 1077–1085 (2005).
37. Hirashima, M., Lu, Y., Byers, L. & Rossant, J. Trophoblast expression of fms-like tyrosine kinase 1 is not required for the establishment of the maternal–fetal interface in the mouse placenta. *Proc. Natl Acad. Sci. USA* **100,** 15637–15642 (2003).
38. Derksen, R. H., Khamashta, M. A. & Branch, D. W. Management of the obstetric antiphospholipid syndrome. *Arthritis Rheum.* **50,** 1028–1039 (2004).
39. Li, Y., Wang, H. Y. & Cho, C. H. Association of heparin with basic fibroblast growth factor, epidermal growth factor, and constitutive nitric oxide synthase on healing of gastric ulcer in rats. *J. Pharmacol. Exp. Ther.* **290,** 789–796 (1999).
40. Girardi, G., Redecha, P. & Salmon, J. E. Heparin prevents antiphospholipid antibody-induced fetal loss by inhibiting complement activation. *Nature Med.* **10,** 1222–1226 (2004).
41. Hills, F. A. *et al.* Heparin prevents programmed cell death in human trophoblast. *Mol. Hum. Reprod.* **12,** 237–243 (2006).
42. Hossain, N., Schatz, F. & Paidas, M. J. Heparin and maternal fetal interface: why should it work to prevent pregnancy complications? *Thromb. Res.* **124,** 653–655 (2009).
43. Girardi, G., Yarilin, D., Thurman, J. M., Holers, V. M. & Salmon, J. E. Complement activation induces dysregulation of angiogenic factors and causes fetal rejection and growth restriction. *J. Exp. Med.* **203,** 2165–2175 (2006).
44. Redecha, P., van Rooijen, N., Torry, D. & Girardi, G. Pravastatin prevents miscarriages in mice: role of tissue factor in placental and fetal injury. *Blood* **113,** 4101–4109 (2009).
45. Myatt, L. & Cui, X. Oxidative stress in the placenta. *Histochem. Cell. Biol.* **122,** 369–382 (2004).
46. Hussain, S. *et al.* Oxidative stress and proinflammatory effects of carbon black and titanium dioxide nanoparticles: role of particle surface area and internalized amount. *Toxicology* **260,** 142–149 (2009).
47. Liu, X. & Sun, J. Endothelial cells dysfunction induced by silica nanoparticles through oxidative stress via JNK/P53 and NF-κB pathways. *Biomaterials* **31,** 8198–8209 (2010).
48. Lundqvist, M. *et al.* Nanoparticle size and surface properties determine the protein corona with possible implications for biological impacts. *Proc. Natl Acad. Sci. USA* **105,** 14265–14270 (2008).
49. Enders, A. C. & Blankenship, T. N. Comparative placental structure. *Adv. Drug Deliv. Rev.* **38,** 3–15 (1999).
50. Rossant, J. & Cross, J. C. Placental development: lessons from mouse mutants. *Nature Rev. Genet.* **2,** 538–548 (2001).

Acknowledgements

This study was supported in part by Grants-in-Aid for Scientific Research from the Ministry of Education, Culture, Sports, Science and Technology of Japan (MEXT) and from the Japan Society for the Promotion of Science (JSPS) through a Knowledge Cluster Initiative (MEXT). It was also supported by Health Labour Sciences Research Grants from the Ministry of Health, Labour and Welfare of Japan (MHLW), by a Global Environment Research Fund from the Minister of the Environment, and by the Food Safety Commission (Cabinet Office), the Cosmetology Research Foundation, the Smoking Research Foundation and the Takeda Science Foundation.

Author contributions

K.Y. and Y.Y. designed the study. K.Y., K.H., K.M., Y. Morishita, M.N., T. Yoshida, T.O., H.N., K.N., Y.A., H.K., Y. Monobe and T.I. performed the experiments. K.Y. and Y.Y. collected and analysed the data. K.Y. and Y.Y. wrote the manuscript. H.A., K.S., Y.K., T.M., S.T., N.I., I.Y., S.S. and T. Yoshikawa provided technical support and conceptual advice. Y.T. supervised the project. All authors discussed the results and commented on the manuscript.

Additional information

The authors declare no competing financial interests. Supplementary information accompanies this paper at www.nature.com/naturenanotechnology. Reprints and permission information is available online at http://npg.nature.com/reprintsandpermissions/. Correspondence and requests for materials should be addressed to Y.Y. and Y.T.

妊娠と免疫

齋藤　滋　　中島彰俊　　島　友子

はじめに

胎児は母親にとって半異物(semiallograft)でもあるにもかかわらず，妊娠は維持される。この際，母体免疫系は胎児(父親)抗原のみ攻撃しない胎児抗原特異的免疫寛容(トレランス)となっている。この機構がうまく働かなくなると，原因不明流産や妊娠高血圧症候群，早産などが引き起こされる。本稿では，まず妊娠維持機構を免疫学的に論じた後に，異常妊娠における免疫学的変化につき概説する。

胎児はなぜ拒絶されないのか

免疫系は自己を攻撃せず，非自己のみを攻撃するが，これは免疫寛容(トレランス)のためと考えられている。胸腺でT細胞が作られる際に，自己と強く反応するT細胞と自己と全く反応しないT細胞はアポトーシスにより除去される。自己と極めて弱く反応し，非自己と強く反応するクローンだけが選択され，自己が守られるようになる。これを中枢性免疫寛容と呼んでいる。しかし中枢性免疫寛容は極めて不備であるため，末梢性免疫寛容というシステムがあり，主として制御性T細胞($CD4^+CD25^+$Treg)がその役割を担っている。癌に対する免疫ができにくいのも末梢性免疫寛容と考えられ，自己免疫疾患では逆に末梢性免疫寛容がうまく働いていないと考えられている。

では，妊娠時には免疫寛容が成立しているのであろうか。**図1**に示すように黒マウス由来の腫瘍細胞を白マウスに移植しても腫瘍は拒絶されてしまう。しかし，あらかじめ黒マウス(♂)と交尾させ白マウスを妊娠させてから黒マウス由来の腫瘍細胞を移植すると，腫瘍は生着し増大する[1]。重要なのは分娩後3週間すると，すべての腫瘍細胞は拒絶されてしまうことである。すなわち，妊娠時のみに父親抗原特異的免疫寛容が成立していることになる。

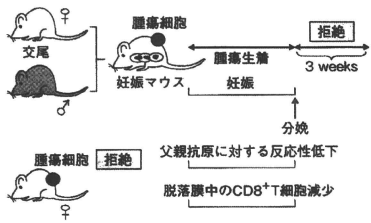

図1　妊娠時には一過性に父親抗原に対する免疫寛容が成立する

最近の研究により，妊娠により制御性T細胞が増加することが判明している[2,3]。T細胞を欠損するBALB/C nu/nuマウスにCD25陰性のリンパ球を移入し(制御性T細胞はCD25を発現しているので，制御性T細胞がない状態)，アロ妊娠させると流産するが，BALB/Cがオスの場合(同一遺伝子妊娠)は流産が起こらないことが報告された[2](**図2**)。制御性T細胞がないため末梢性免疫寛容が働かず異物である胎児が拒絶されたと解釈された。ほかの研究において抗CD25抗体を用いてCD25を発現している細胞を除去すると，アロ妊娠の際，着床障害や流産が起こることが報告されてお

さいとう しげる，なかじま あきとし，しま ともこ
富山大学産科婦人科学教室
〒930-0194　富山県富山市杉谷2630
E-mail address：s30saito@med.u-toyama.ac.jp

表1　妊娠時における NK 細胞分画の変化[5]

	CD94 Inhibitory receptor	Ly49	ASGM-1	CD25	CD122	Thy-1^{lo}	c-kit^{lo}
BALB/C							
非妊末梢血	48.2±3.8	76.4±5.0	91.7±2.2	5.0±1.2	89.2±8.4	16.1±4.2	2.2±0.5
妊娠末梢血（13日目）	83.0±3.4	74.3±4.1	95.3±4.3	3.2±2.0	69.5±2.8	21.9±3.2	1.8±0.4
妊娠子宮（13日目）	80.7±7.4	84.2±6.5	86.6±5.4	87.3±6.7	85.2±4.3	30.9±2.9	13.3±2.4
NOD/SCID							
非妊末梢血	0.4±0.2	10.3±2.8	83.8±3.5	1.9±1.5	44.9±4.2	41.8±4.1	90.7±4.0
妊娠末梢血（13日目）	5.5±3.3	12.1±2.6	93.5±2.5	2.3±1.9	45.4±6.3	92.9±1.6	81.1±3.1
妊娠子宮（13日目）	43.8±4.3	5.2±5.0	73.8±6.1	84.7±5.2	59.5±6.5	85.9±3.3	93.3±3.4

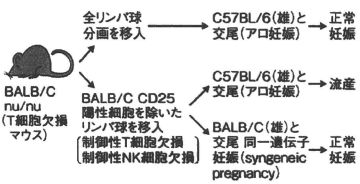

図2　制御性T細胞はアロ妊娠維持には必要である

り，制御性T細胞は着床にも関与すると考えられる[4]。しかし，最近の筆者らの研究で，NK 細胞にも CD25 を発現する細胞があり，CD25$^+$NK 細胞は妊娠子宮で増加し（**表1**），免疫を制御する IL-10 や TGF-β を産生することが判明した[5]。NOD/SCID マウスは T 細胞，B 細胞を欠くマウスで NK 細胞機能不全を有している。BALB/C マウスでも NOD/SCID マウスでも妊娠子宮に特異的に CD25 陽性細胞が増加している。さらに CD4$^+$CD25$^+$制御性T細胞のみを除去したマウスを作製し，アロ妊娠させると流産率が高まるが，妊娠子宮由来の CD25$^+$NK 細胞を移入すると流産が減少することも見いだした[6]。すなわちアロ妊娠維持には制御性T細胞のみならず CD25$^+$制御性 NK 細胞が重要であることが判明した。

各種病態における免疫環境

1．着床障害

マウスでは妊娠 4.5 日目で着床するが，すでに妊娠 2.5 日目の子宮領域リンパ節では父親抗原特異的な制御性 T 細胞が増加している[7]。また妊娠 2.5 日目に抗 CD25 抗体を投与して制御性 T 細胞と制御性 NK 細胞を除去すると，着床障害が起こることから[4]，免疫寛容が着床にも重要な役割を果たすことがマウスで明らかになっている。しかしヒト着床不全では未だ報告がなく，今後解明すべき点であろう。しかし，ヒト原因不明不妊症例での子宮内膜での Foxp3 mRNA（Foxp3 は制御性T細胞の分化誘導因子）が低下していることは報告されている[8]。

2．流産

流産例や習慣流産例の末梢血や脱落膜（子宮内膜）での制御性T細胞率は減少しており（**表2**），また習慣流産例の制御性 T 細胞機能も低下している[9]。しかし，制御性 NK 細胞についての研究は全くなされていない。

それでは，ヒト流産で免疫細胞が胎児や絨毛を攻撃している証拠はあるのであろうか。胎児，胎盤を攻撃するリンパ球は CD8$^+$T細胞もしくは NK 細胞である。これらの細胞は顆粒中に perforin，

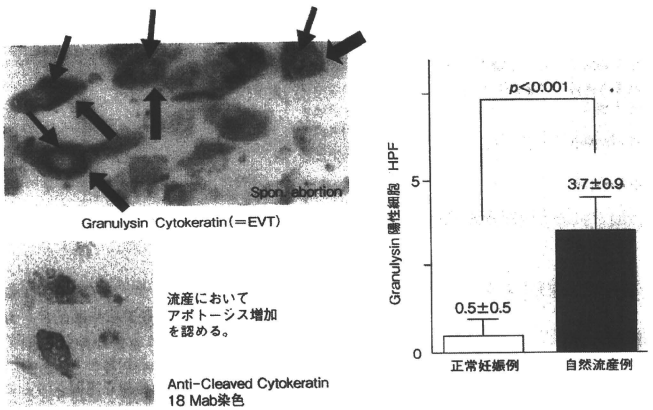

図3　流産症例のEVTの核はGranulysin陽性となりアポトーシスに陥る

表2　妊娠時におけるCD4$^+$CD25$^+$制御性T細胞率
(Sasaki ら, 2004)[3]

	制御性CD4$^+$CD25^{bright}/CD4率(%)
非妊婦	
末梢血(n=10)	6.50±0.59
子宮内膜(n=2)	6.07±0.14
妊娠初期	
末梢血(n=20)	8.51±2.48*
子宮内膜(n=20)	21.84±2.92**
自然流産	
末梢血(n=9)	5.66±1.58
子宮内膜(n=9)	7.14±1.85
習慣流産	
末梢血(n=4)	6.16±4.58
子宮内膜(n=4)	6.24±0.99

*p<0.05 vs non-pregnancy PBL, **p<0.0001 vs non-pregnancy PBL vs sp-ab. decidua vs hab-ab. decidua

granzyme, granulysin などの細胞傷害をきたす分子を内蔵しており，標的細胞は，これらの分子により細胞死を引き起こす。流産症例でこれらの分子の発現を免疫組織学的検討，flow cytometry にて検討したところ，流産例の脱落膜には granulysin 陽性の NK 細胞が増加していることを見いだした[10]。さらに興味あることに，流産例の絨毛外トロホブラスト(extravillous trophoblast)の核に granulysin が染色され，それらの細胞はアポトーシスを起こして死んでいることが判明した(**図3**)。GFP 遺伝子と連結した granulysin 発現ベクターを用いて細胞内の granulysin を可視化したところ，細胞質内の granulysin が 48 時間以降核内に集まり，その後細胞死が起こることが証明された[10]。すなわち，ヒト流産において母体免疫細胞は流産の際に胎児を攻撃していることが初めて明らかとなった。このことより，一層，免疫寛容が妊娠維持に重要な役割を果たすと考えられる。

3．分娩前後での制御性T細胞の変動

末梢血中の制御性T細胞は妊娠初期から増加し始め，妊娠中期で最高値をとり，以後漸減していく[11]。妊娠末期になり分娩が近づくにつれ制御性T細胞(CD4$^+$CD25^{high})が減少し，活性化T(CD4$^+$CD25^{low})細胞が増加する[12]。また分娩時の制御性T細胞は経腟分娩時のほうが，予定帝王切開分娩時より低いので[13]，制御性T細胞の減少が子宮局所内での免疫細胞を活性化させて，分娩(胎児拒

表3　正常妊娠と合併症での免疫系の変化

	正常分娩	絨床不全	正常妊娠	流産	妊娠高血圧腎症	早産
制御性T細胞	増加	?	増加	減少	減少	?
父親抗原特異的制御性T細胞	増加(マウス) ヒトでは?	?	増加(マウス) ヒトでは?	減少(マウス) ヒトでは?	?	?
制御性NK細胞	?	?	増加(マウス) ヒトでは?	?	?	?
NK細胞活性化	?	?	抑制	活性化 絨毛傷害	活性化	?
Th1/Th2バランス	Th2優位	Th1優位	Th2優位	Th1優位	Th1優位	Th2優位

絶)が起こっているのかもしれない。

4. 妊娠高血圧症候群

妊娠高血圧腎症(PE)は妊娠時の高血圧と蛋白尿を合併する疾患であるが，初産婦に多い，経産婦でもパートナーが変わると初回妊娠時に高率となる，パートナーが同じでも最終分娩から10年以上経過するとPEのリスクは初産婦と同様になることが知られている[14]。免疫寛容に働く制御性T細胞はメモリー機能を有しており数年間は生存する。したがって2回目の妊娠時でパートナーが同じであれば即座に父親抗原特異的制御性T細胞が増加して，十分な免疫寛容を誘導するが，パートナーが変わった際や，10年以上最後の分娩から経過すると父親抗原特異的制御性T細胞(メモリーT細胞)が初回妊娠時と同じレベルまで低下してしまい，PEの発症リスクは初回妊娠時と変わらなくなると理解することができる。精漿中には可溶性の父親MHC抗原が含まれるが，同棲期間が短かったり，ハネムーンベイビーでは精液曝露期間が短いため父親抗原に対する免疫寛容が不十分でPEになるとも考えられる[14]。また胎児は通常であれば半分は自己で半分が非自己となるsemiallograftであるが，第三者からの胚を代理母に移植する際は，完全なallograftとなり，より強力な免疫寛容が必要となる。この場合のPEの発症率は25%と極めて高く[15]，免疫寛容とPEとの関連性が示唆される疫学的な事象となっている。

現在のところ父親抗原特異的制御性T細胞を評価できる表面マーカーはないが，PEでは制御性T細胞が末梢血のみならず子宮内においても低下することが報告されている[16]。またPEでは免疫系が活性化されており，拒絶反応に関与するTh1免疫優位となっていることも知られている[17]。PEの際，全身の炎症性反応が亢進しているが，慢性的な炎症は制御性T細胞機能を減弱させることも報告されており，制御性T細胞の減少と機能不全の二つがPEの病態に深く関与していると考えられる。

5. 早産

早産例では高率に絨毛膜羊膜炎(CAM)が合併しており，子宮内感染が病態と深く関与している。当然のことながら好中球や単球は活性化しており，卵膜破壊やプロスタグランジン産生増加により前期破水や子宮収縮を引き起こす。この際，Th17細胞が増加し，産生されるIL-17はTNFαによる卵膜間質細胞からのIL-8産生を増強する[18]。すなわちT細胞も局所の炎症増強に作用している。興味あることにTh17細胞と制御性T細胞は同一のprogenitor cellから分化するため，Th17細胞が増加することは制御性T細胞が減少していることを示唆する。また早産時の子宮局所の炎症は制御性T細胞の機能を減弱させることが示唆されるが，未だ直接証明した報告はない。

おわりに

表3に産科的合併症時における免疫系の変化をまとめた。各種合併症を免疫系の異常として捉えると，異なった視点から治療戦略がみえてくる。また制御性NK細胞については全く手つかずの状

況であるので，これから多くの知見が望まれる。

文献

1) Tafuri A, Alferink J, Möller P, et al：T cell awareness of paternal alloantigens during pregnancy. Science **270**：630–633, 1995
2) Aluvihare VR, Kallikourdis M, Betz AG：Regulatory T cells mediate maternal tolerance to the fetus. Nat Immunol **5**：266–271, 2004
3) Sasaki Y, Sakai M, Miyazaki S, et al：Decidual and peripheral blood CD4+CD25+regulatory T cells in early pregnancy subjects and spontaneous abortion cases. Mol Hum Reprod **10**：347–353, 2004
4) Shima T, Sasaki Y, Itoh M, et al：Regulatory T cells are necessary for implantation and maintenance of early pregnancy but not late pregnancy in allogeneic mice. J Reprod Immunol **85**：121–129, 2010
5) Lin Y, Zhong Y, Saito S, et al：Characterization of natural killer cells in nonobese diabetic/severely compromised immunodeficient mice during pregnancy. Fertil Steril **91**：2676–2686, 2009
6) Saito S, Shima T, Nakashima A, et al：The role of regulatory NK and regulatory T cells in the maintenance of pregnancy. J Reprod Immunol **86**：17, 2010
7) Robertson SA, Guerin LR, Bromfield JJ, et al：Seminal fluid drives expansion of the CD4+CD25+ T regulatory cell pool and induces tolerance to paternal alloantigens in mice. Biol Reprod **80**：1036–1045, 2009
8) Jasper MJ, Tremellen KP, Robertson SA：Primary unexplained infertility is associated with reduced expression of the T-regulatory cell transcription factor Foxp3 in endometrial tissue. Mol Hum Reprod **12**：301–308, 2006
9) Arruvito L, Sanz M, Banham AH, et al：Expansion of CD4+CD25+ and FOXP3+ regulatory T cells during the follicular phase of the menstrual cycle：implications for human reproduction. J Immunol **178**：2572–2578, 2007
10) Nakashima A, Shiozaki A, Myojo S, et al：Granulysin produced by uterine natural killer cells induces apoptosis of extravillous trophoblasts in spontaneous abortion. Am J Pathol **173**：653–664, 2008
11) Somerset DA, Zheng Y, Kilby MD, et al：Normal human pregnancy is associated with an elevation in the immune suppressive CD25+CD4+ regulatory T-cell subset. Immunology **112**：38–43, 2004
12) Zhao JX, Zeng YY, Liu Y：Fetal alloantigen is responsible for the expansion of the CD4(+)CD25(+) regulatory T cell pool during pregnancy. J Reprod Immunol **75**：71–81, 2007
13) Sindram-Trujillo AP, Scherjon SA, van Hulst-van Miert PP, et al：Comparison of decidual leukocytes following spontaneous vaginal delivery and elective cesarean section in uncomplicated human term pregnancy. J Reprod Immunol **62**：125–137, 2004
14) Saito S, Shiozaki A, Nakashima A, et al：The role of the immune system in preeclampsia. Mol Aspects Med **28**：192–209, 2007
15) Salha O, Sharma V, Dada T, et al：The influence of donated gametes on the incidence of hypertensive disorders of pregnancy. Hum Reprod **14**：2268–2273, 1999
16) Sasaki Y, Darmochwal-Kolarz D, Suzuki D, et al：Proportion of peripheral blood and decidual CD4(+)CD25 (bright) regulatory T cells in pre-eclampsia. Clin Exp Immunol **149**：139–145, 2007
17) Saito S, Sakai M：J Th1/Th2 balance in preeclampsia. Reprod Immunol **59**：161–173, 2003
18) Ito M, Nakashima A, Hidaka T, et al：A role for IL-17 in induction of an inflammation at the fetomaternal interface in preterm labour. J Reprod Immunol **84**：75–85, 2010

* * *

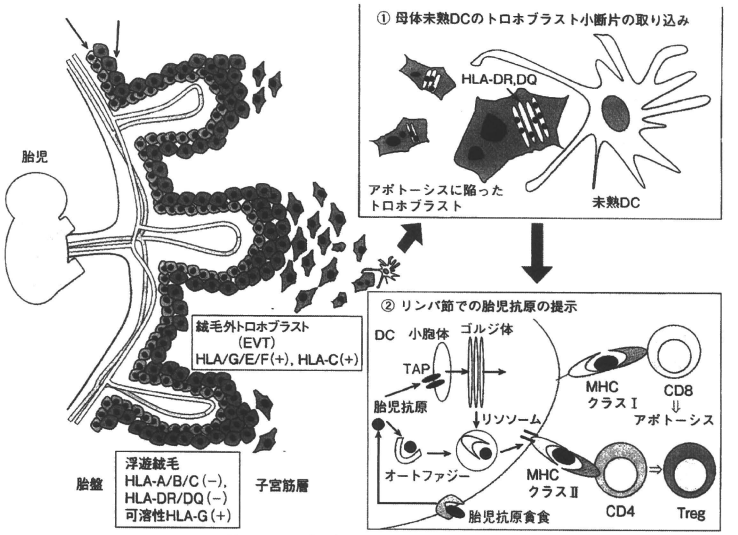

図1　DCによる胎児組織の認識，抗原提示

細胞様の細胞が増加するが，妊娠中期以降は減少する。遺伝子改変によりNK細胞を欠くマウスを作製し，このマウスを妊娠させると，脱落膜は空虚となり血管壁も厚くなり，胎盤への血流が減少する。このことにより，NK細胞は脱落膜のらせん動脈の形成に重要な役割を果たすと考えられるようになってきている。ヒトの場合，NK細胞は，末梢血では$CD16^+$NK細胞が主体で，$CD16^-CD56^{bright}$NK細胞は1%にも満たないが，子宮内膜中のNK細胞は$CD16^-CD56^{bright}$NK細胞(uNK)が主体を占め，しかも，増殖期子宮内膜，分泌期子宮内膜，妊娠初期脱落膜の順に増加し，妊娠初期脱落膜では60〜70%を占めるようになる[1]。反復流産患者の分泌期中期の子宮内膜を生検するとuNK細胞が減少しており，$CD16^+$NK細胞，$CD8^+$T細胞，B細胞が増加するという報告がある。また，原因不明習慣流産患者の脱落膜中のuNK細胞は正常妊娠に比較して低率となっている。

これら脱落膜中のuNK細胞はトロホブラストに対し細胞傷害活性を示さないことが知られている。また，NK細胞は，自身のもつ活性型および抑制型レセプターによって，その細胞傷害活性が制御され，EVTに発現しているHLA-C，HLA-E，HLA-Gはこれらレセプターの特異的なリガンドである(**図2**)。

NK細胞上のCタイプレクチン型のヘテロ二量体であるCD94/NKG2のうち，CD94/NKG2Aは抑制型レセプターであり，HLA-Eを認識し，このシグナルにより細胞傷害能が抑制される。逆に，CD94/NKG2Cは活性型レセプターであり，HLA-Eを認識し，このシグナルにより細胞傷害能が活性化される(**表1**)。末梢血NK細胞上には両者が存在するが，脱落膜中のuNK細胞では，すべてのNK細胞が抑制型レセプターであるNKG2Aを発現しており，約70%が$NKG2A^+NKG2C^-$，約30%が$NKG2A^+NKG2C^+$である[2]。

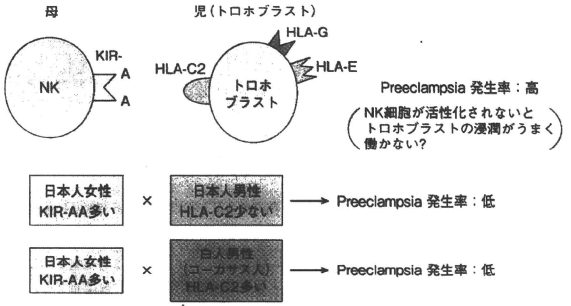

図2　母親 NK 細胞上の KIR-AA 発現と児の HLA-C2 との関連

表1　NK 細胞上のレセプターと胎児側の組織適合性抗原との関係

NK 細胞上レセプター	EVT 上の分子
抑制型レセプター	
CD94/NKG2D	HLA-E
KIR2DL2/3(KIRA)	HLA-C1
KIR2DL1(KIRA)	HLA-C2
ILT2	HLA-G
活性型レセプター	
CD94/NKG2C	HLA-E
KIR2DL4	HLA-G(?)
KIR2DS(KIRB)	HLA-C
NKG2D	MICA/B, ULBP

すなわち，uNK 細胞は NK 活性化レセプターを細胞表面に表出している場合でも，常に NK 細胞を抑制するシグナルが存在することにより EVT 上の HLA-E を認識してもトロホブラスト細胞を攻撃しなくなると考えられる[3]。

HLA-G は NK 細胞上に発現している免疫グロブリンスーパーファミリーに属するキラー細胞免疫グロブリン様レセプター(killer immunoglobulin-like receptor：KIR)の中の KIR-2DL4，あるいは免疫グロブリン様転写産物(immunoglobulin-like transcript：ILT)に認識される(表1)。KIR-2DL4 は活性レセプターであり，IFN-γの産生を誘導するが NK 細胞の細胞傷害活性は亢進させない。また，HLA-G テトラマーは KIR2DL4 と結合することができず，uNK を活性化させないと考えられている。ILT に関しては機能面では未だ不明の点が多い。

EVT 上に発現する HLA-C は多型性を示し，HLA-C1 および HLA-C2 に大別される。HLA-C は KIR により認識される。KIR は活性化シグナルを欠く KIR-A と，活性化レセプターである KIR-B に大別される。Hiby ら[1]は，母親の KIR のタイピングと胎児の HLA-C のタイピングを行い，胎児の HLA-C が C2 で母体の KIR が KIR-AA 遺伝子型であると妊娠高血圧腎症のリスクが高くなることを報告した。すなわち，母体の NK レセプターの遺伝子型と胎児の HLA-C の遺伝子型の組合せが妊娠高血圧腎症のリスクになるといえる(図2)。

日本人は KIR-AA が世界で最も高頻度の民族(ほぼ60%)であるが，HLA-C2 は世界で最も頻度が低い(約10%)。これにより妊娠高血圧腎症の発症リスクがコントロールされている可能性がある(図2)。ヨーロッパのコーカサス人(白人)は KIR-AA 型が20～30%，HLA-C2 型が20～30%とともに中程度である。したがって，日本人女性(KIR-AA 高頻度)と白人男性(HLA-C2 中頻度)が結婚して妊娠した際，妊娠高血圧腎症は理論上3～4倍に増加することになる(図2)。そこで，筆者らは実際に国際結婚による症例を324症例集めて妊娠高血圧腎症の発症率を調査したが，初産(発症率2.0%)でも経産(発症率0.8%)でも，日本

人同士のカップルと頻度に差を認めず[5]，疫学的にHibyらのデータを追認することはできなかった。このことはNK細胞だけで胎盤での母児免疫寛容を説明することは不十分であり，NK細胞以外のメカニズム，すなわちT細胞による免疫寛容誘導が関与しているためではないかと考えられる。事実，最近になり母体T細胞は胎児の発現するHLA-Cを認識しておりHLA-Cのミスマッチ(不適合)がある場合，T細胞は活性化されており，それに伴って免疫を抑制する制御性T細胞が脱落膜で増加していることが明らかとなっている。これらについて次項で述べる。

脱落膜における制御性T細胞の働き

T細胞は細胞性免疫を司るTh1細胞と液性免疫を司るTh2細胞に大別される。母体のTh1とTh2細胞のバランスは妊娠維持機構に関与し，正常妊娠ではTh2細胞優位の状態が誘導されているという報告が多く，胎盤局所におけるTh2サイトカイン優位の状態が妊娠維持に有利に働くと考えられてきた。しかし，Th2サイトカインであるIL-4，IL-5，IL-9，IL-13をノックアウトしたマウスでもアロ妊娠が成立することなどから，最近ではほかの免疫系の関与，すなわち制御性T細胞(regulatory T cell：Treg)の関与が考えられるようになってきた。

Treg細胞は末梢性の免疫寛容の維持に重要な役割を果たしている細胞集団で，自己反応性T細胞の免疫反応の抑制に働く。それ以外にも，腫瘍免疫，移植免疫，アレルギー，微生物感染などの多様な免疫反応に及ぶことが示唆されており，マウスアロ抗原特異的に免疫反応を制御し，$CD4^+CD25^+$T細胞の分画に存在する。また，Treg細胞は，核内転写因子のFoxp3がマスター遺伝子であり，ヒトのTreg細胞はCD25を強発現する$CD4^+CD25^{bright}$細胞である。これまでの報告により，Treg細胞は胎児母体間の免疫寛容においてもキーファクターとなり得ることが示唆されている(**表2**)。ヒト[6]，マウスともに妊娠時には脱落膜(子宮内膜)や末梢血中にTreg細胞が増加しており，流産モデルマウス，ヒト反復流産症例，ヒト妊娠高血圧症候群症例ではTreg細胞数の減少が認められている。また，原因不明不妊の子宮内膜ではFoxp3のmRNA発現レベルが減少しているという報告もある。我々も，マウスにおいて妊娠2.5日目に抗CD25モノクローナル抗体(PC61)を投与し$CD4^+CD25^+$Treg細胞を減少させるとアロ交配では着床が起こらず，同系交配では着床が成立すること，また，妊娠4.5日目および7.5日目の抗CD25モノクローナル抗体投与ではアロ交配において流産率が上昇することを確認している[7]。すなわち，制御性T細胞はアロ妊娠において着床成立，妊娠初期における妊娠維持になくてはならない細胞である。

ヒトの母子間でHLA-Cミスマッチが存在すると脱落膜中の$CD4^+CD25^{dim}$活性化T細胞が増加し，$CD4^+CD25^{bright}$Treg細胞が増加する。Tilburgsら[8]は母体のT細胞はトロホブラスト上のHLA-Cを認識しており，胎児抗原特異的にTreg細胞の抑制能を発揮することを報告している。このことは，ヒトでも母親T細胞は胎児抗原を認識し活性化されるが，制御性T細胞が過剰な活性化を局所で制御していることを示す。また，Robertsonら[9]はマウスの系で，精巣でプライミングすることにより父親抗原を認識するTreg細胞が妊娠3.5日目に子宮所属リンパ節に集積し，父親抗原特異的な免疫寛容(父親由来腫瘍細胞接種による腫瘍の増

表2　妊娠と制御性T細胞の関係

病態	制御性T細胞(Treg)の変動
正常妊娠	末梢血や脱落膜ともに増加する，特に脱落膜で著明に増加。母子間のHLA-Cミスマッチがあると脱落膜でさらに増加
原因不明不妊症	子宮内膜で低下(Foxp3mRNAのみの成績で実際にはTreg細胞数を検討していない)
着床不全	着床期にTregを減少させると着床できない
原因不明流産，不育症	子宮内膜で低下，妊娠初期にTreg減少させると流産が誘導される
妊娠高血圧腎症	末梢血，脱落膜ともに減少
早産	？
妊娠糖尿病	*in vitro*で培養するとTreg減少

大，父親由来リンパ球投与による遅延型過敏反応の増強)を誘導することを報告している。すなわちTreg細胞は胎児抗原(あるいは父親抗原)を認識しており，着床前から子宮の所属リンパ節に集簇，着床後は子宮に移動し，胎児抗原特異的に免疫寛容を誘導しているということがいえる。

脱落膜における樹状細胞(DC)の働き

ヒトでは非妊娠子宮内膜分泌期後期ではほかの月経周期や妊娠初期に比較し，$CD83^+$成熟DCが増えている[10]。一方，妊娠初期脱落膜に存在するDCの大部分がC型レクチンであるDC-SIGN，CD209を高発現した未熟DCである[1]。$DC\text{-}SIGN^+$未熟DCは貪食作用活性は十分高いが，T細胞の活性化能は不十分である。先に胎児と母体間に起こっている細胞の交通(microchimerism)に言及したが，妊娠中，母体血液中には大量のシンシトロホブラストの微小片が循環している。このトロホブラストの細胞残骸内の微小片にはHLA-DRおよびDQといったMHCクラスⅡ抗原が発現されており，母体未熟DCはこれを取り込み抗原処理しMHCクラスⅠ分子あるいはクラスⅡ分子上に提示する。また，トロホブラストから遊離したエクソソーム上に発現する胎児抗原もDCに取り込まれMHCクラスⅠ抗原もクラスⅡ抗原も抗原提示される。一般にIL-10存在下では抗原特異的制御性T細胞が誘導されやすい。正常妊娠の場合，胎盤やNK細胞からIL-10が産生されており，IL-10に反応したDCは末梢での制御性T細胞を誘導している可能性がある[11]。また，MHCクラスⅠ抗原は母体$CD8^+$T細胞に認識され，$CD8^+$T細胞は活性化されるが，活性化$CD8^+$T細胞はトロホブラストが発現するFasLによりアポトーシスに陥る。また，脱落膜中のNK細胞から産生されるガレクチン1は活性化$CD8^+$T細胞をアポトーシスに陥らせる。つまり，胎児抗原を認識した活性化$CD8^+$T細胞はアポトーシスにより除去されるため，胎児を攻撃できない。

また，脱落膜中のDCはT細胞との相互作用の結果，Th1/Th2タイプ免疫反応を誘導することはよく知られているが，子宮内に存在するDCも局所のTh1/Th2バランスをTh2に傾け妊娠維持に働いている[12]。

最近，ジフテリアトキシンを投与することにより免疫過程で$CD11c^+$細胞を取り除くことが可能なCD11c－DTRトランスジェニックマウスが開発された。着床期において一時的に$CD11c^+$DCを除去すると着床率が著しく低下することが証明された。着床部のuterine NK(uNK)細胞の成熟化も障害され，脱落膜内のらせん動脈の発達や胎盤の発育が障害された[13]。DCは抗原提示細胞であるため，母体T細胞へ胎児抗原が提示されることが妊娠に必須である可能性も考えられたが，T細胞を欠損するマウスや同系交配においてもDCを着床期に除去すると着床不全が生じた。このことは制御性T細胞除去はアロ妊娠の着床不全を誘導するが同系妊娠では誘導しないことと大きく異なる。Plackらによると，DCには血管新生を誘導する作用を認めており，DCは着床時の血管新生を誘導することで着床成立に関与している可能性があるといえる。以上より，DCは着床やその後の胎盤形成に重要な役割を果たしているといえる。

胎盤から分泌されるエクソソーム[14]

細胞間の情報伝達の新しいメカニズムとして近年，エクソソーム(exosome)の研究が盛んになってきている。エキソソームとは血液，リンパ球，体液に存在する，直径50～100 nmの膜で包まれた小胞のことであり，細胞膜から分泌されている。抗原提示細胞から分泌されるエキソソームは，MHC class Ⅰ，Ⅱを膜表面にもち，T細胞を活性化することが知られている。また，上皮細胞や腫瘍細胞などから分泌されるエキソソームは免疫抑制活性をもつことが報告されている。最近，ヒトの胎盤から分泌されるエキソソームについての報告もされるようになってきた。エクソソームは従来報告されていたトロホブラストの小断片よりはるかに小さい。ヒトの胎盤由来のエキソソームにはMHCクラスⅠ関連分子のMICA，MICBやRetinoic acid early transcript 1 proteins(ULBP)をもちNKG2Dレセプターを介してNK細胞の活性化を抑制している。また，アポトーシスを誘導す

るFAS-LやTRIRを発現し，$CD8^+$細胞などのアポトーシスを引き起こしていると考えられている。

これらのことからトロホブラスト由来エキソソームは免疫抑制活性をもち，母児境界面での免疫寛容に一役かっているといえる。

おわりに

妊娠成立時の母児接点の場では，胎児抗原の制御，母体免疫担当細胞などいくつかの免疫寛容の機構が相互に作用していることが最近の生殖免疫学の進歩により明らかとなってきた。免疫学的維持機構の破綻と原因不明の着床不全，反復流産，妊娠高血圧腎症といった疾患の関連性が報告されている。今後，さらなる研究が発展し，これらの疾患に対して新たな治療法が開発されることに期待したい。

文献

1) Saito S, et al : Cytokine network at the feto-maternal interface. J Reprod Immunol **47** : 87–103, 2000
2) Kusumi M, et al : Expression patterns of lectin-like natural killer receptors, inhibitory CD94/NKG2A, and activating CD94/NKG2C on decidual $CD56^{bright}$ natural killer cells differ from those on peripheral $CD56^{dim}$ natural killer cells. J Reprod Immunol **70** : 33–42, 2006
3) Tabiasco J, et al : Human decidual NKcells : unique phenotype and functional properties. Placenta **27** : 4–9, 2006
4) Hiby S, et al : Combinations of maternal KIR and fetal HLA-C genes influence the risk of preeclampsia and reproductive success. J Exp Med **200** : 957–965, 2004
5) Saito S, et al : The incidence of pre-eclampsia among couples consisting of Japanese women and Caucasian men. J Reprod immunol **70** : 93–98, 2006
6) Sasaki Y, et al : Decidual and peripheral blood $CD4^+$ $CD25^+$ regulatory T cells in early pregnancy subjects and spontaneous abortion. Mol Hum Reprod **10** : 347–353, 2004
7) Shima T, et al : Regulatory T cells are necessary for implantation and maintenance of early pregnancy but not late pregnancy in allogeneic mice. J Reprod Immunol **85** : 121–129, 2010
8) Tilburgs T, et al : Fetal-maternal HLA-C mismatch is associated with decidual T cell activation and induction of functional T regulatory cells. J Reprod Immunol **82** : 148–157, 2009
9) Robertson SA, et al : Seminal fluid drives expansion of the $CD4^+CD25^+$ T regulatory cell pool and induces tolerance to paternal alloantigens in mice. Biol Reprod **80** : 1036–1045, 2009
10) Rieger L, et al : Antigen-presenting cells in human endometrium during the menstrual cycle compared to early pregnancy. J Soc Gynecol Investig **11** : 488–493, 2004
11) Adams K, et al : The changing maternal self hypothesis : A mechanism for maternal tolerance of the fetus : Placenta **28** : 378–382, 2007
12) Miyazaki S, et al : Predominance of Th2-promoting dendritic cells in early human pregnancy deciduas. J Leuko Biol **74** : 514–522, 2003
13) Krey G, et al : *In vivo* dendritic cell depletion reduces breeding efficiency, affecting implantation and early placental development in mice. J Mol Med **86** : 999–1011, 2008
14) Mincheva-Nilsson L, et al : The role of placental exosomes in reproduction. Am J Reprod Immunol **63** : 520–533, 2010

* * *